Gas and solid behaviours during defluidisation of Geldart-A particles

E.T. Santos [a,b,*], M. Hémati [a], R. Andreux [b], G. Ferschneider [b]

[a] Laboratoire de Génie Chimique de Toulouse UMR 5503, INP-ENSIACET, 4 Allée Emile Monso, BP 44362, 31030 Toulouse, Cedex 4, France
[b] IFP Energies nouvelles, BP3, 69360 Solaize, France

A B S T R A C T

Bed collapsing experiments were carried out in a cold-air transparent column 192 mm in diameter and 2 m high. Typical Fluid Catalytic Cracking (FCC) catalyst with a mean particle size of 76 μm and a density of 1400 kg/m^3 was used. Both single and double-drainage protocols were tested. The local pressure drop and bed surface collapse height were acquired throughout the bed settling.

Typical results were found regarding dense phase voidage of a fluidised bed and the bed surface collapse velocity. In addition, bubble fraction was calculated based on the collapse curve.

Experimental results showed that windbox effect is significantly reduced compared to previous works since the volume of air within the windbox was reduced. The comparison of single/double-drainage protocols revealed a new period in the defluidisation of Geldart-A particles concerning gas compressibility. Through the temporal analysis of local pressure drop, the progress of the solid sedimentation front from bottom to top was determined, analysed and modelled.

1. Introduction

The downward convey of gas–solid dense mixtures in standpipes is a major issue in the Fluid Catalytic Cracking (FCC) process, which is traditionally the major conversion unit of heavy liquid oils to lighter and more valuable gas products in a refinery. The dense transport can be best achieved whilst maintaining the particles in a moderately aerated state with interstitial gas. The aerated gas-particle suspension behaves as a fluid, thus the pressure along the vertical pipe increases. The static pressure head is directly related to the apparent density of the suspension and the height of the pipe. Standpipe flows are certainly the most illustrative case of this wide family of two-phase gas–solid dense downward flows. Many authors have experimentally studied these flows, underlying that the powders fluidity is a key point in processes involving gas–solid streams [1-3].

Due to the pressure build-up that compresses the interstitial gas, the fluidised behaviour of the downward flow cannot be maintained unless additional gas is injected through aeration taps positioned along the standpipe. However, the injected gas flow rates can cause instabilities: either local gas-particle flow deaeration when the injected gas flow rates are too low, or appearing of stagnant gas voids when the injected gas flow rates are too high [1]. These two phenomena are respectively described as the local defluidisation and the local over-aeration. Based on the analysis of the gas/solid slip velocity, deduced from local pressure gradient measurements, Leung and Wilson [4] showed that standpipe flows can be described in different regimes such as moving bubbling fluidised bed, a moving homogeneous fluidised bed, or a moving packed bed that rubs against the internal wall of the standpipe. As a matter of fact, the gas–solid flow can eventually switch from one regime to the other from the top to the bottom of the standpipe, depending on the solid mass flux, the distance between each aeration tap, and the aeration gas flow rates [5, 6]. Thus, the behaviour of the moving gas-particle suspension under successive over- and under-aeration is a key parameter for the control and the stability of the flow. The knowledge of the characteristic times of the deaeration, the voidage of the suspension, the bubble velocity and void fraction in case of heterogeneous fluidisation, is critical. However, because defluidisation and refluidisation are hard to investigate in the "real condition" standpipe flow, the study in a static fluidised bed is a straightforward manner to observe, describe, understand, and model the driving basic mechanisms.

One of the most standard techniques is the single-drainage bed collapse technique, used to determine the voidage and gas velocity of the dense phase and bubble fractions in gas–solid fluidised beds of fine powders [7-14]. It consists of fluidising a given powder, cutting-off the fluidisation gas supply, and then measuring the collapsing bed height and the pressure drop generated by the exiting interstitial gas across the bed. It has been shown that the effect of the residual gas exiting from the windbox through the bed cannot be neglected, and improvements of the bed collapse technique have been proposed. They consist either in modifying the equations for the voidage and gas velocity of the dense phase [10] or in performing the dual-drainage bed collapse technique [15]. The previous studies focused on the effects of the (i) physical properties of the powders (diameter, density, percentage of fines),

* Corresponding author at: Laboratoire de Génie Chimique de Toulouse UMR 5503, INP-ENSIACET, 4 Allée Emile Monso, BP 44362, 31030 Toulouse, Cedex 4, France. Tel.: +33 5 34 32 36 81; fax: +33 5 34 32 36 97.
E-mail address: edgar.tavaresdossantos@ensiacet.fr (E.T. Santos).

(ii) the bed height, (iii) the distributor (porous or perforated plate), (iv) windbox volume, (v) operating pressure, (vi) fluidising velocity before defluidisation. It was shown that the dynamic deaeration behaviour (voidage of the emulsion phase, bubble fraction, deaeration time) strongly depends on the initial state of the bed; i.e. homogeneously or heterogeneously fluidised. Moreover, deaeration occurs with two propagation front lines: a downward at the surface of the bed corresponding to the exiting of gas phase, and an upward at the distributor relative to the compaction of the solid phase which was never studied systematically.

This study focuses on the deaeration behaviour of the FCC powder in a static fluidised bed under operating conditions representative of the continuous standpipe flows. The aim of this work is to describe, quantify, and model, the effects of the driven parameters. Both single- and double-drainage techniques are used: the former models the standpipe flow when local deaeration occurs with only upwards interstitial gas leakage; the latter when it occurs with upwards and downwards interstitial gas leakage.

1.1. State of the art of the bed collapse technique results

A typical defluidisation collapse curve is shown in Fig. 1. The fluidised bed collapse is composed of three zones: bubble escape (zone 1); dense phase sedimentation (zone 2) and consolidation (zone 3). In most reported cases, when the air is suddenly cut-off, the bed surface initially collapses as bubbles rise up to the bed surface. The bed height then decreases at a constant rate as the particles sedimentation takes place until the bed level stabilisation.

Two parameters can be determined from the defluidisation curve analyses (Fig. 1) [9]:

- the height of the dense phase, H_D, of the fluidised bed is obtained by extrapolating to zero time the sedimentation slow settling rate. The voidage of the dense phase, ε_D, is determined by means of a mass balance:

$$\varepsilon_D = 1 - \frac{m_p}{\rho_p A H_D} \tag{1}$$

where m_p represents the mass of particles in the bed, ρ_p the particles density and A the cross-sectional area of the column;

- the dense phase gas velocity, u_D, is given by the slope of the collapse curve, u_c [13]. Tung and Kwauk [10], in analogy with the sedimentation theory, showed that the deaeration velocity is the same as that of the dense phase velocity of a fluidised bed. However, one should consider the existence of other proposed methods to calculate u_D from the voidage/velocity curve [9] or using a Richardson–Zaki equation type: $u_D = u_t \varepsilon_D^n$, with u_t the particle terminal velocity value and n an exponent characteristic to each powder [9].

1.2. Gas behaviour during defluidisation

Most bed collapse experiments have been carried out using a single drainage method in which residual gas in the bed and windbox is drained through the bed. In this case, the effect of the residual gas flow from the windbox through the bed cannot be neglected in the bed collapse measurements by the single drainage method [15]. To assess this contribution, Tung and Kwauk [10] corrected the collapsing bed level velocity, u_c, with the gas leakage velocity from the windbox, u_w, using the following expression:

$$u_w = \frac{\left(\frac{W}{A} + \Delta P_d\right) H_w}{P_a t_c} \tag{2}$$

where W represents the weight of the powder in the bed, A the cross-sectional area of the column, H_w the height of the windbox, ΔP_d the pressure drop through the distributor, P_a the atmospheric pressure and t_c the time instant at the end of zone 2 (Fig. 1).

The double drainage method was also studied [15, 16]. Rowe et al. [17] reported that the exact values of the voidage and the gas velocity of the dense phase can be obtained only if the pressure of the windbox is reduced to zero as soon as possible as the fluidising gas is shut-off which was not the case of most previous works in the literature [15]. Park et al. [15] evaluated the effect of the residual gas volume in the windbox and proposed an optimum dual-drainage method.

1.3. Solid behaviour during defluidisation

Visual observations of a 2D transparent fluidised moke-up allowed Geldart and Wong [13] to conclude the existence of a 2-front solid displacement during defluidisation: one corresponding to bed surface collapse and another corresponding to solid upward sedimentation (Fig. 1).

The upward sedimentation front has not been the subject of many studies and information on this phenomenon is still missing. Regarding its velocity, the development of the Engelhard test provided the first data [18]. The test consists in measuring the required time for the pressure measured 30.48 cm above the distributor to start decreasing after the air supply is cut-off. The test presents some limitations

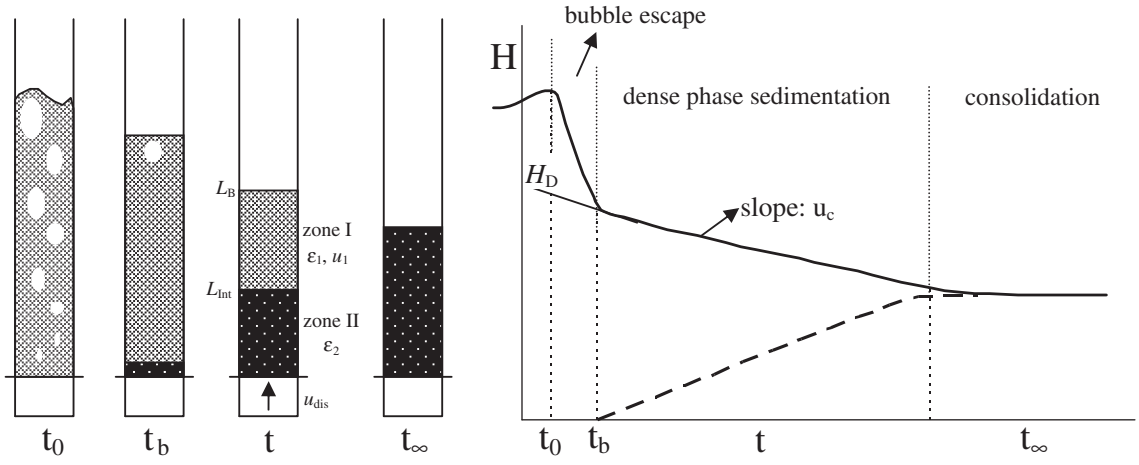

Fig. 1. Typical stages and analysis of Geldart-A FCC catalyst defluidisation curve: schematic of the 2-front solid displacement during defluidisation [13].

Table 1
FCC catalyst physical properties.

Powder	Cracking catalyst
Particle mean diameter, d_p (μm)	76
Apparent density, ρ_p (kg/m^3)	1400
Bulk density, ρ_b (kg/m^3)	818
Tapped density, ρ_{tap} (kg/m^3)	936
Repose angle (°)	29

due to its intrusive character and the poor estimation of the sedimentation front using only one point. Also, when the measured pressure is zero one part of the bed above the captor is already in a fixed bed state. To overcome this factor, Sharma et al. [18] have defined the defluidisation time (transition from fluidised to fixed bed), from the pressure drop temporal data, as the first observed slope changing.

1.4. Objectives

Even though the bed collapse test has been the subject of numerous studies, some additional knowledge and characterisation can be obtained when analysing the temporal local pressure drop signal. This new information can be used to transpose this static phenomenon to the dynamics of gas–solid dense downward flows. Moreover, the experimental results were successfully modelled using the interpretation of Cherntongchai and Brandani [19] for the bed collapse experiment. The aim of this work is, therefore, to provide new relevant understanding of the defluidisation of Geldart-A particles, such as the FCC catalyst, to later transpose to the complexity of the downward gas–solid dense phase flows.

2. Experimental

2.1. Materials

Typical FCC particles were used. Physical properties are given in Table 1. The catalyst has a size distribution between 10 and 200 μm. The mean particle diameter is 76 μm and its density of 1400 kg/m^3 therefore belonging to the group A of the Geldart classification [20].

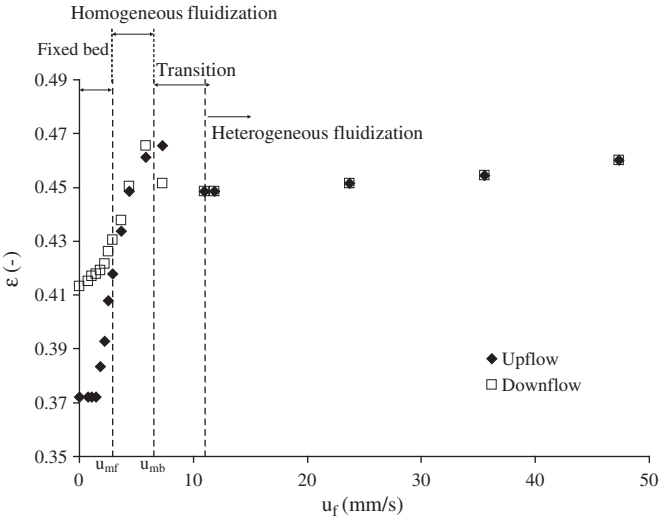

Fig. 2. FCC catalyst fluidisation curve.

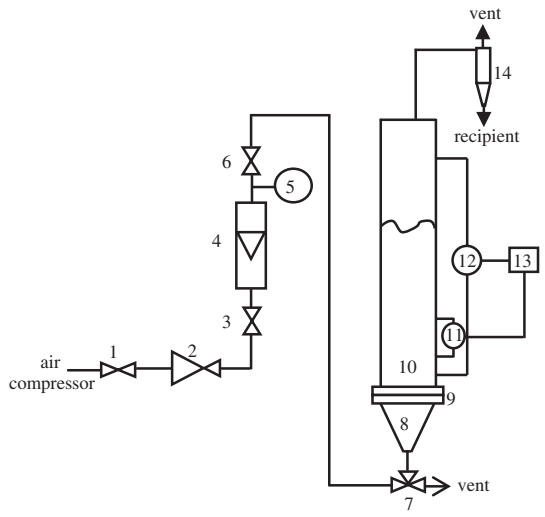

Fig. 3. Drawing of the experimental apparatus. Legend: 1—valve; 2—pressure regulator; 3—valve (single-drainage method); 4—rotameter; 5—manometer; 6—valve; 7—three-way valve (double-drainage method); 8—windbox; 9—distributor; 10—fluidised bed; 11—local pressure transducers; 12—total pressure transducer; 13—recorder; 14—cyclone.

Fluidisation properties (u_{mf}; u_{mb}; ε_{mf}; ε_{mb}) were determined experimentally in a classic fluidised bed using different bed weights (7 kg; 14 kg and 21 kg). The minimum fluidising velocity was determined using the Richardson method [21]. The fluidisation regimes were identified plotting the bed mean voidage against the gas velocity (Fig. 2). The typical regimes were identified [9]:

- fixed bed: $u_f < u_{mf}$;
- homogeneous fluidisation: $u_{mf} < u_f < u_{mb}$;
- transition: $u_{mb} < u_f < 1.5\ u_{mb}$;
- heterogeneous fluidisation: $u_{mb} < u_f$.

2.2. Experimental apparatus

Bed collapse experiments were carried out in a cold-air transparent Plexigas column 192 mm in diameter and 2 m high. A cyclone is placed at the top to collect the entrained solids as shown in Fig. 3. Since the ratio of the column diameter to the mean particle diameter

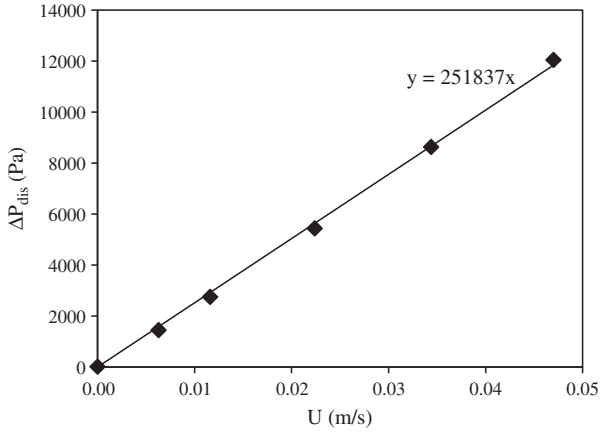

Fig. 4. Experimental characterisation of the distributor.

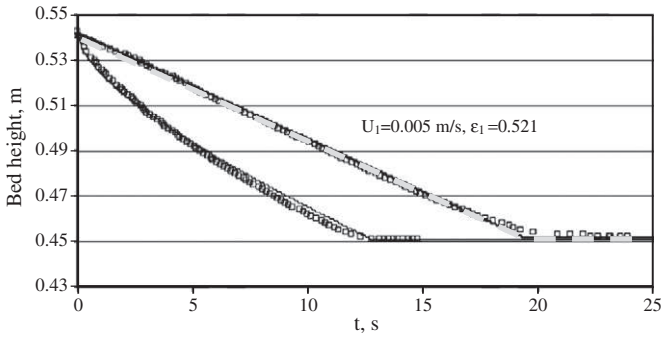

Fig. 5. Model validation with Cherntongchai and Brandani [19] results. (—) this work.

is larger than 2500, the possible wall effects can be neglected in the present experiments.

The pressure drop across the porous distributor is found to be linear relatively to the gas velocity and is of 1559 Pa when fluidising at 1.2 cm/s (Fig. 4).

The gas phase, air from an oil-free compressor, is fed to the bed through a pressure regulator, a calibrated rotameter that provides a fluidising velocity, u_f, between 1 mm/s and 80 mm/s, a conical shape windbox ($D_w = 19$ cm; $H_w = 19$ cm) and a porous distributor. The relative humidity of the air is 30%.

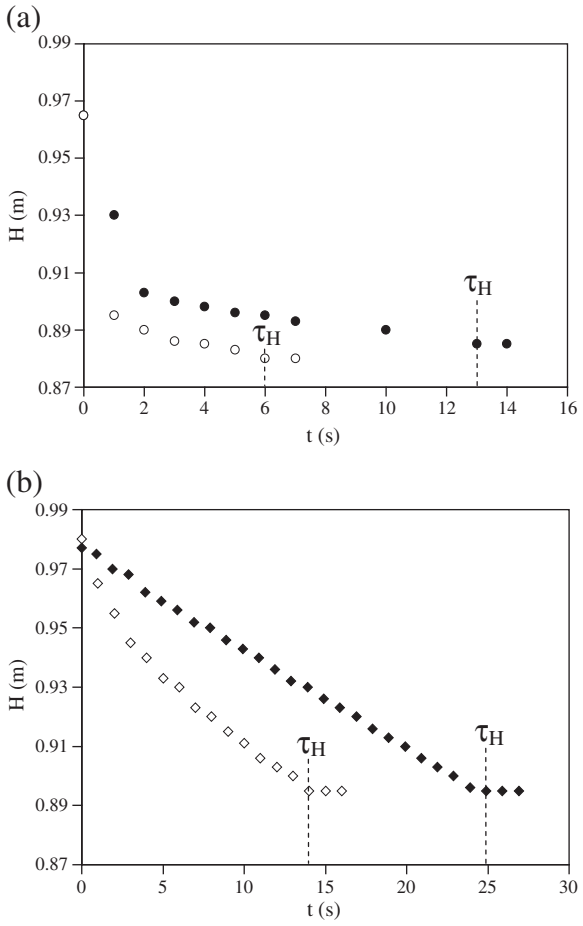

Fig. 6. Evolution of the bed height with time during defluidisation, single (filled)/double drainage method comparison. $H_0 = 885$ mm. (a) (●,○) $u_f = 47.4$ mm/s, $\frac{u_f}{u_{mb}} = 7.29$; (b) (◊,♦) $u_f = 6.3$ mm/s, $\frac{u_f}{u_{mb}} = 0.97$.

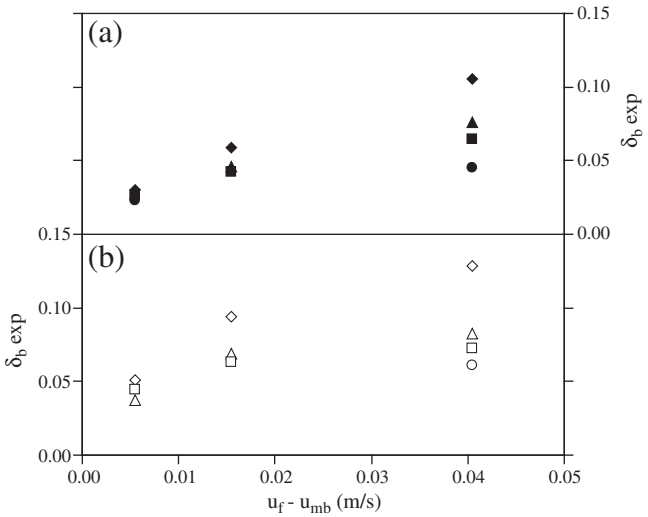

Fig. 7. Effect of fluidising velocity, u_f–u_{mb}, on the fraction of bubbles in the bed. (a) Single drainage; (b) double drainage. (♦) $H_0 = 0.300$ m; (▲) $H_0 = 0.597$ m; (■) $H_0 = 0.885$ m; (●) $H_0 = 0.915$ m.

A ruler was placed on the wall of the column to measure the expanded and collapsing bed heights. Local and global pressure drop was measured using pressure transducers. The pressure data was acquired with a sampling frequency, f, of 10 Hz.

2.3. Procedure

Initially a known weight of solids (7.02 kg; 14.14 kg; 21.12 kg and 21.50 kg) was loaded into the column providing four different static bed heights: 300 mm; 597 mm; 885 mm and 915 mm. The powder was then fluidised by the compressed air at the desired superficial velocity ($u_{mb} < u_f < 8\ u_{mb}$).

When the system reached a steady-state (pressure fluctuations irrespective of time) the air supply was suddenly cut-off. Single and double drainage protocols were then applied. To evaluate the single drainage method, the air supply was cut-off at the rotameter (Fig. 3) thus forcing the residual air to be purged through the bed of particles. Double drainage method was studied by cutting off the air at the

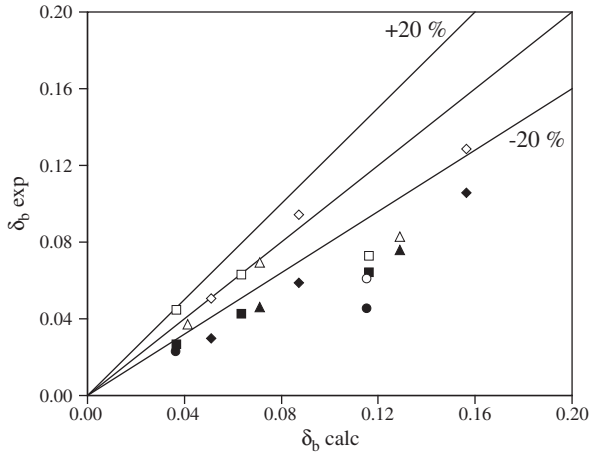

Fig. 8. Comparison between theoretical and experimental fraction of bubbles in the bed. Single (filled)/double drainage. (♦) $H_0 = 0.300$ m; (▲) $H_0 = 0.597$ m; (■)$H_0 = 0.885$ m; (●) $H_0 = 0.915$ m.

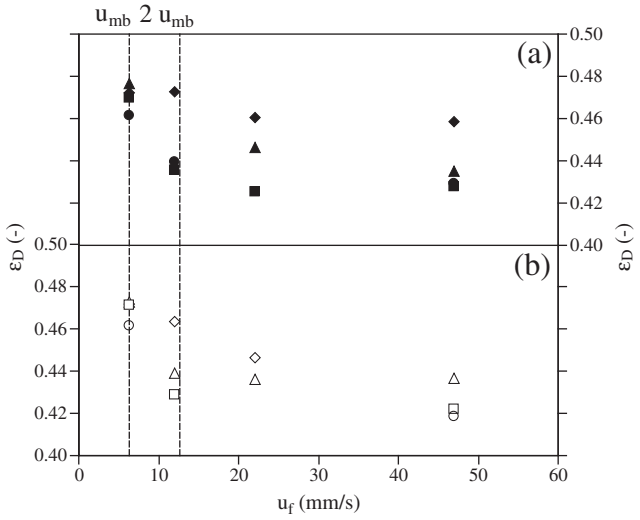

Fig. 9. Effect of fluidising velocity, u_f–u_{mb}, on the dense phase voidage. (a) Single drainage; (b) double drainage. (♦) $H_0 = 0.300$ m; (▲) $H_0 = 0.597$ m; (■) $H_0 = 0.885$ m; (●) $H_0 = 0.915$ m.

entrance of the windbox through a three-way valve (Fig. 3) placing both column bottom and top at atmospheric pressure.

The bed height, recorded with a digital camera at 25 fps, and pressure drop ($f = 10$ Hz) were acquired simultaneously during the defluidisation phenomena.

3. Modelling

The experimental results were modelled based on the model proposed by Cherntonghai and Brandani [19]. The main assumptions and equations of the model detailed in [19] are presented hereunder:

1. One-dimensional system;
2. In the bed sections, the fluid is incompressible;
3. Negligible inertial effects;
4. $t>0$, $u_{dis} \leq u_{mf}$;
5. The top fluidised section remains at a constant void fraction ε_1 corresponding to a gas velocity u_1 (Fig. 1);
6. The gas in the windbox is compressible and is considered ideal.

From the solid and gas-phase mass balance the following equations were deduced:

$$\frac{dL_B}{dt} = u_{dis} - u_1 \tag{3}$$

$$\frac{dL_{Int}}{dt} = \frac{1-\varepsilon_1}{\varepsilon_2-\varepsilon_1}\frac{dL_B}{dt} \tag{4}$$

where L_B is the height of the collapsing bed, L_{Int} the height of zone II, u_{dis} the superficial velocity of the gas flowing through the distributor, ε_1 and ε_2 the porosities of zones I and II, respectively (Fig. 1).

The problem is closed with an equation for the distributor velocity:

$$-\frac{dP_w}{dt} = \frac{P_w}{V_w} u_{dis} A \tag{5}$$

where P_w is the absolute pressure in the windbox, V_w the windbox volume and A the cross-sectional area. The distributor velocity, u_{dis} is calculated based on the pressure drop across the distributor, ΔP_d (Fig. 4).The ΔP_d is determined evaluating the momentum balance:

$$\Delta P_d = (P_w - P_{atm}) - \rho_f g L_B - \Delta P_1 - \Delta P_2 \tag{6}$$

where ΔP_1 corresponds to the pressure drop in zone I, fluid-particle system at equilibrium, ΔP_2 the zone II fixed bed pressure drop function of u_{dis}, determined with experimental results or Ergun modified law as presented in [19].

The bubble escape stage was introduced performing a total mass balance over the control volume and assuming that the bubbling zone properties are similar to the stationary bubbling fluidised bed, giving the following equation:

$$\frac{dL_{Tot}}{dt} = u_{dis} - u_f. \tag{7}$$

The developed model was tested using the parameters provided in [19]. Fig. 5 shows, as expected, that the present model predicts the same behaviour. To be noted that only the single drainage experiments were modelled since the discharge valve was not characterised.

4. Results and discussion

4.1. Bed collapse curve

The collapsing behaviour previously reported by Geldart and Wong [13] was observed: typical single drainage bed collapse curves composed of bubble escape, particle sedimentation and bed consolidation periods were obtained when the initial gas velocities were above the minimum bubbling state (Fig. 6.a). When the fluidising velocity was at the minimum bubbling state, only constant rate sedimentation and consolidation periods were found (Fig. 6.b).

Double drainage method showed a decrease of the total surface settling time, τ_H, for the two initial bed structures studied: homogeneous and heterogeneous. This results in a faster bed surface collapse

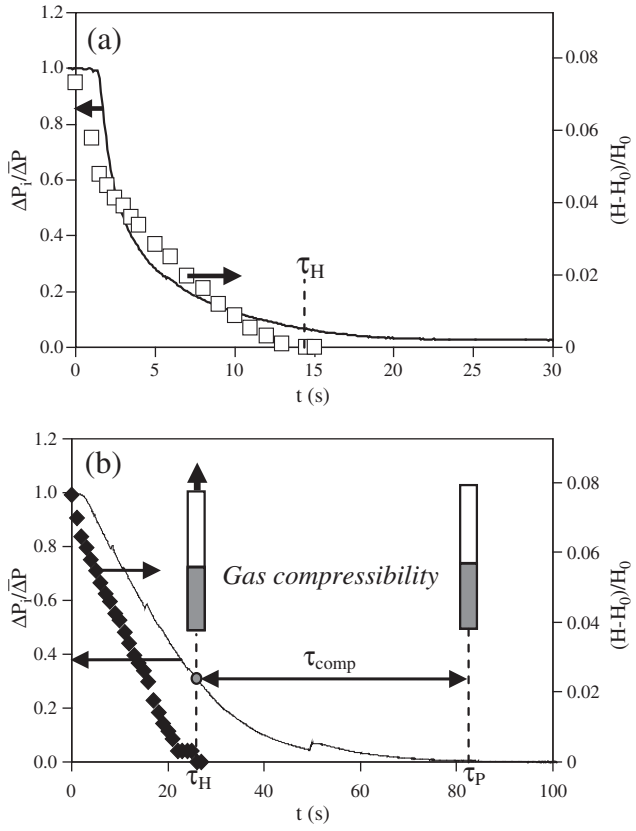

Fig. 10. Gas compressibility effect. (a) Double drainage; (b) single drainage. $H_0 = 915$ mm; $u_f = 6.3$ mm/s.

rate, as well as a smaller bed height, thus evacuating more interstitial gas within the bed. Also, the bed surface collapse is rather parabolic than linear in the case of a homogeneous fluidised bed (Fig. 6).

4.2. Fluidised bed initial condition effect

4.2.1. Homogeneous fluidised bed

Concerning the homogeneous fluidised bed, the abrupt collapse of the bed is not observed: the dense phase voidage, ε_D, is equal to the bed voidage, ε. Moreover, the voidage decreases at a constant rate with time consequently resulting in a fairly constant collapsing bed surface velocity, u_c, with a mean value of 3.5 mm/s using the single drainage method. This value is in agreement with previously reported values by Geldart and Radtke [1] and Geldart and Wong [13] for powders with similar physical properties.

The use of the double drainage method resulted in a 30% increase of the collapsing velocity, u_c, due to the escape of gas through the distributor.

4.2.2. Heterogeneous fluidised bed

From the zone 1 of the collapse curve (Fig. 6.a), the fraction of bubbles in the bed was determined using the following equation:

$$\delta_b = \frac{H_i - H_{tr}}{H_i} \tag{8}$$

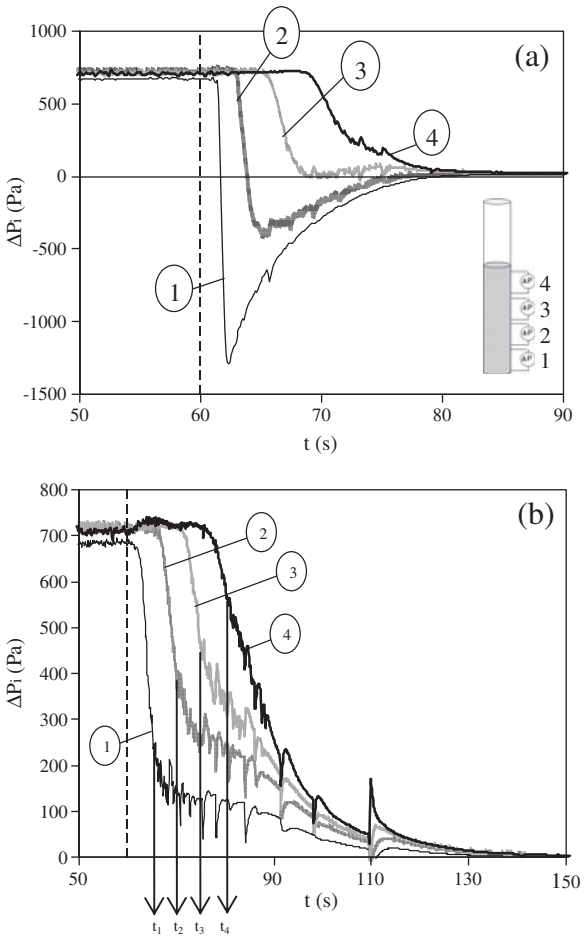

Fig. 11. Local pressure drop temporal evolution during defluidisation. (a) Double drainage; (b) single drainage. ΔP_1: 115–215 mm; ΔP_2: 315–415 mm; ΔP_3: 515–615 mm; ΔP_4: 715–815 mm.

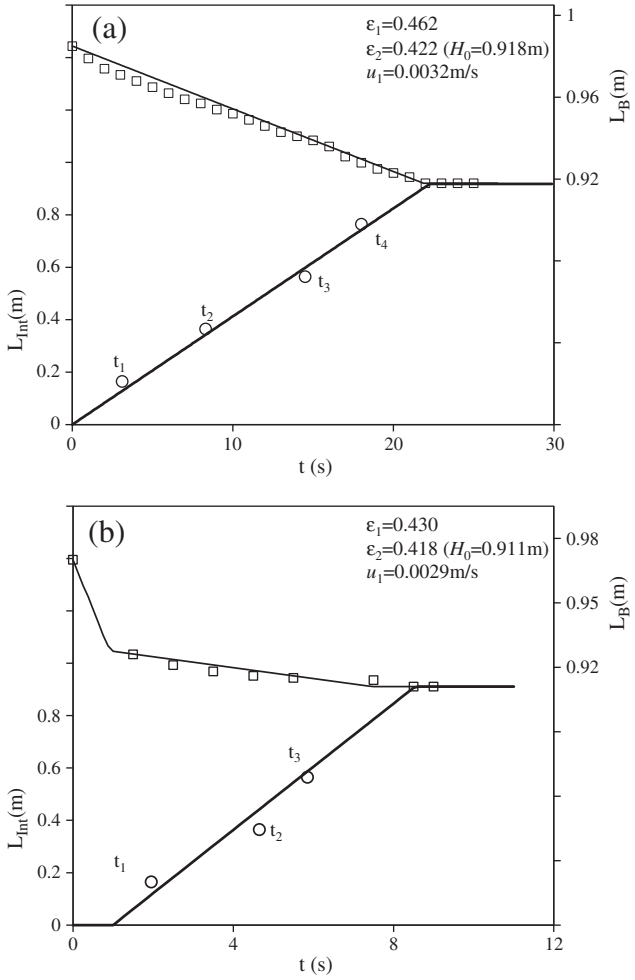

Fig. 12. Model fit of single drainage experiments: (a) $u_f = 6.3$ mm/s; (b) $u_f = 47.4$ mm/s. Points: experimental; Lines: model.

where H_i represents the mean bed height before defluidisation and H_{tr} the transition height from bubble escape to dense phase sedimentation.

According to Fig. 7, increasing the fluidising velocity leads to an increase of the fraction of bubbles in the bed. This was observed for all of the tested bed heights.

Moreover, for a given fluidising velocity, increasing the bed height leads to a decrease of the bubble fraction in the bed (Fig. 7). These results can be explained by the influence of the bed height on bubble diameter and velocity. Indeed, the increase of bed height will lead to an augmentation of bubble size and velocity which will cause a decrease in the fraction of bubbles as shown by the following expressions:

$$\delta_b = \frac{u_f - u_{mb}}{U_b} \tag{9}$$

where U_b is the bubble velocity given by

$$U_b = u_f - u_{mf} + 0.711\sqrt{g\overline{d_b}} \tag{10}$$

The mean bubble diameter, $\overline{d_b}$, can be estimated, according to Mori and Wen [21], through the expression:

$$\overline{d_b} = d_m - (d_m - d_{b0})\, exp\left[-0.3\,\frac{H_i}{2D}\right] \tag{11}$$

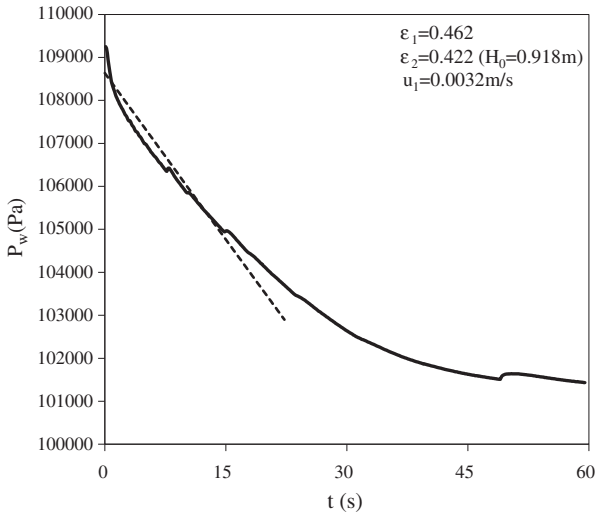

Fig. 13. Evolution of the absolute pressure in the distributor during defluidisation for single drainage and $u_f = 6.3$ mm/s: (—) experimental; (––) model.

where D represents the column diameter, d_m, the maximal theoretical bubble diameter, which is given by

$$d_m = 1.64\left[A\ \left(u_f - u_{mb}\right)\right]^{0.4} \quad (12)$$

and d_{b0}, the bubble initial diameter, by

$$d_{b0} = 0.915\cdot 10^{-2}\left(u_f - u_{mb}\right)^{0.4}. \quad (13)$$

From the previous set of equations, the theoretical fraction of bubbles was calculated. Fig. 8 shows that predictions are not accurate for experiments using single drainage method as well as for high fluidising velocities. The discrepancies in the results come from:

- the fact that correlations proposed by Mori and Wen [22] are adapted to Geldart-B particles;
- the uncertainty in measuring the bed height in zone 1. Indeed, it has already been reported the difficulty in analysing images of heterogeneous fluidised beds [9].

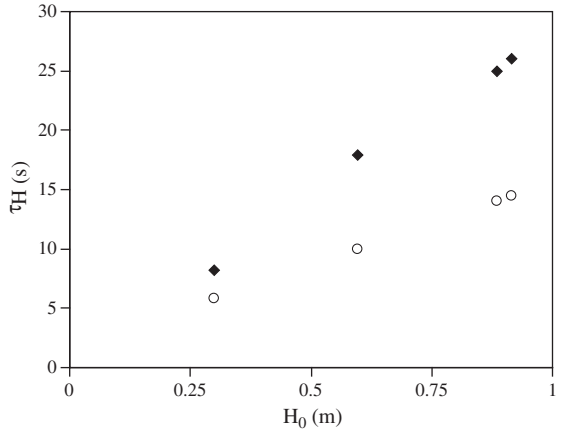

Fig. 14. Effect of the initial bed height, H_0, on the surface settling time, τ_H. $u_f = 6.3$ mm/s. (♦) Single drainage; (○) Double drainage.

Table 2
Comparison of the solid sedimentation front velocity.

Drainage	H_0/τ_H (mm/s)	$u_{s,0}$ (mm/s)	Error (%)
Single	35	38	−8
Double	59	68	−13

Typical results were found concerning the fluidising velocity influence on the dense phase voidage [9, 11, 13]. For instance, the results found in this work are identical to those obtained by Barreto et al. [11] when studying the fluidising velocity effect on the dense phase voidage by means of X-ray absorption and bed collapse technique for similar powders. Fig. 9 shows that the dense phase voidage:

- decreases rapidly for fluidising velocities between u_{mb} and 1.5 u_{mb};
- decreases with the augmentation of the bed height.

The bubble size dependence of gas fluidising velocity and bed height explains these results. In fact, the increase of the bubble size leads to a compression of the interstitial gas by the bubbles, leading to a less aerated and more compacted suspension.

Empirical correlations are proposed for the two evacuation methods in study:

- single drainage:

$$\varepsilon_D = 0.38\,u_f^{-0.035}H_0^{-0.051}, 6\ \text{mm/s} \le u_f \le 50\ \text{mm/s}, 2 \le H_0/D \le 6 \quad (14)$$

- double drainage:

$$\varepsilon_D = 0.36\,u_f^{-0.046}H_0^{-0.032}, 6\ \text{mm/s} \le u_f \le 50\ \text{mm/s}, 2 \le H_0/D \le 6 \quad (15)$$

Regarding zone 2, dense phase sedimentation, the collapsing velocity decreases with the augmentation of the fluidising velocity and bed height. Again, the fluidising velocity and the bed height are key parameters in the aeration state of the dense phase of a fluidised bed. Moreover, the increase of fluidisation velocity and bed height and the subsequent increase of bubble rising velocity leads to the formation of a less aerated dense phase presenting higher resistance to the evacuation of the interstitial gas. From the experimental data the following correlations were proposed:

- single drainage:

$$u_c = 0.0012\,u_f^{-0.18}H_0^{-0.23}, 6\ \text{mm/s} \le u_f \le 50\ \text{mm/s}, 2 \le H_0/D \le 6 \quad (16)$$

- double drainage:

$$u_c = 0.0014\,u_f^{-0.21}H_0^{-0.19}, 6\ \text{mm/s} \le u_f \le 50\ \text{mm/s}, 2 \le H_0/D \le 6. \quad (17)$$

Notice that the exponent of the bed height parameter is similar to the one proposed by Abrahamsen and Geldart [9]: $u_c \propto H^{-0.244}$ (18).

4.3. Gas compressibility effect

A new trend, never reported in the literature, is observed when plotting simultaneously the normalised total bed pressure drop and the normalised collapse bed level during the defluidisation by a single

drainage method which is not observed when using the double drainage method. Indeed, Fig. 10 shows the existence of a period during which the pressure drop across the bed is positive whilst the bed of particles is completely settled. Therefore, a gas stream passes through the bed during this period whilst defluidisation (sedimentation of solid particles) is complete. This can be explained by the expansion of the interstitial gas in the bed once the defluidisation is complete. In this case, the gas compression is a non-negligible phenomenon, despite the small dimensions of the bed.

A new characteristic time, τ_{comp}, is defined between the complete bed settling (τ_H) and the zero pressure drop (τ_P) times (Fig. 10). This time is related to the gas compressibility and characterises the decompression of the interstitial gas in the fixed bed. The slope changing in the global pressure drop curve corresponds to the complete settling of the bed of particles (Fig. 10). In addition, the gas velocity in the dense phase cannot be estimated by the slope of the collapsing bed level [7, 8, 13, 23] since the surface collapse curve is also affected by the gas compressibility during defluidisation.

4.4. Solid behaviour during defluidisation

Local pressure drop measurements during the bed defluidisation showed that a fast defluidisation of the middle of the bed first occurs when using a double-drainage protocol (Fig. 11.a). Also, negative local pressure drop values are observed in the bottom of the bed hence air escapes through the windbox. The gas escaping through the windbox eliminates the compressibility period observed when using a single-drainage method (Fig. 11.b).

Local pressure drop data of single drainage experiments show a transition point (Fig. 11.b), as previously reported (Fig. 10). This transition point takes place when the bed settling is complete. Transposing this observation, the local pressure drop data underlines the existence of a front of solids displaced from the bottom to the top of the column reaching the surface when the bed settling is complete. This phenomenon, already described by Geldart and Wong [13] using a black-lighted two-dimensional bed defluidisation experiments, was never properly quantified.

The temporal analysis of local pressure drop can determine the progress of the sedimentation front of the solid particles in the defluidisation. It was considered that the moment when the oscillations of the local pressure drop begin is associated with the complete settling of particles in the bed, as shown in Fig. 11.

4.5. Modelling

Fig. 12.a compares the experimental and simulated results for a homogeneous fluidised bed using the single drainage method. The model satisfactorily predicts the two characteristic fronts of defluidisation using the initial and final voidage values for zones I (ε_1) and II (ε_2). The velocity in the fluidised zone (u_1) is similar to the minimum fluidising velocity (0.003 m/s). Moreover, the pressure in the windbox is suitably described until the beginning of the compressible stage (Fig. 13).

The heterogeneous fluidised bed is also correctly described by the model (Fig. 12.b). The voidage of the fixed bed zone (ε_2) is calculated by a mass balance with the height of the settled bed and the values of u_1 and ε_1 correspond to the minimum fluidising conditions.

The results corroborate the previous findings that: the heterogeneous structure leads to a compression of the interstitial gas by the exiting of bubbles, leading to a less aerated and more compacted suspension.

The local pressure drop analysis and the sedimentation front issued from the simulation results are in agreement. Therefore, the local pressure drop signal analysis may be a powerful tool for phenomena identification in standpipe dysfunction.

4.6. Bed height influence on homogeneous fluidised beds

Fig. 14 shows that, in the presence of a homogeneous fluidised bed, the surface collapse settling time increases linearly with the static bed height. This indicates the constant settling rate of the bed surface throughout defluidisation. Moreover, this linear evolution of τ_H with the static bed height is observed for the two drainage methods: single and double.

Double drainage method removes the effect of the gas contained in the windbox. Then, if with the single drainage method the same linear evolution with bed height is observed, it can be concluded that the same phenomena are present. Thus, the influence of the gas contained in the windbox can be neglected in the present defluidisation experiments. This is related to the reduction in the windbox volume to the fluidised bed air volume ratio by using a conical shaped windbox, 48% with $H_0 = 300$ mm and 16% with $H_0 = 915$ mm when compared to previous works where it represented between 60% and 330% [15, 23].

Furthermore, the time required for the complete settling of the surface is equal to the time required for the sedimentation front to go from 0 to H_0. Thus, the velocity of the ascending sedimentation front can be calculated by: $u_{s,0} = \frac{H_0}{\tau_H}$ (19). The results are presented in Table 2. The values determined by the two methods are concordant (temporal analysis of local pressure drop data and using Eq. (19)).

Finally, the characteristic sedimentation rate of a Geldart-A particles homogeneous fluidised bed can be calculated by simple laboratory experiments through the determination of the total surface collapse time for different static bed heights. Moreover, this velocity can be used to estimate the maximal solid flux in a non-aerated standpipe. In such flows the descending velocity of the particles should be higher than the solid sedimentation ascending front.

5. Conclusion

The aim of the present work was to provide new relevant information on the defluidisation of Geldart-A particles to later transpose to downward gas–solid dense flows. Experimental observations showed the typical collapsing behaviour. The findings regarding the dense phase voidage of a fluidised bed and the bed surface collapse velocity are in agreement with the two-phase theory and with previous authors' reports for fluidising velocities higher than the minimum bubbling velocity. Moreover, the fraction of bubbles was calculated based on the collapse curve. Results are also in agreement with two phase theory and the use of fast camera image analysis to this end may lead to improvements on the determination of bubble properties.

The existence of a gas compressibility period was described through the simultaneous analysis of both surface collapsing level and pressure drop measurements. Moreover, the definition of the gas velocity in a dense phase fluidised bed, reported to be given by the slope of the surface collapse curve, is not accurate. Thus, to characterise this parameter, a new fundamental test must be found or the validation of numerical simulation must be used.

Through the temporal analysis of local pressure drop the progress of the solid sedimentation front from bottom to top was determined. The velocity of the ascending sedimentation solid front is ten times superior to the collapse of the bed surface.

The experimental results were fitted using the model proposed by [19]. The bed height collapse is correctly described and the upward sedimentation front is similar to the one determined through the local pressure drop analysis. The local pressure drop signal analysis may provide new information on standpipe flows dysfunction phenomena identification.

List of symbols

A	cross-sectional area of column, m^2
d_b	bubble mean diameter, m

d_{b0} bubble initial diameter, m
d_m maximal theoretical bubble diameter, m
d_p particle mean diameter, μm
D column diameter, m
f acquisition frequency, Hz
g gravity, m/s^2
$H(t)$ collapsing bed height at time, t
H_0 static bed height, m
H_D dense phase bed height, m
H_i initial bed height, m
H_R air humidity, %
H_{tr} height at defluidised free bubble bed, m
H_w windbox height, m
L_B height of the collapsing bed, m
L_{Int} height of zone II, m
L_{Tot} height of the bubbling fluidised bed, m
m_p mass of particles, kg
n exponent in Richardson–Zaki equation, (−)
P_a atmospheric pressure, Pa
P_w windbox absolute pressure, Pa
t time, s
t_c required time to start consolidation, s
U_b bubble velocity, mm/s
u_1 emulsion phase superficial velocity in zone I, mm/s
u_c collapsing bed surface velocity, mm/s
u_D dense phase gas velocity, mm/s
u_{dis} superficial velocity of gas flowing through the distributor, mm/s
u_f fluidising velocity, mm/s
u_{mb} minimum bubbling velocity, mm/s
u_{mf} minimum fluidising velocity, mm/s
$u_{s,0}$ homogeneous bed sedimentation solid front velocity, mm/s
V_w windbox volume, m^3
W weight of powder in the bed, N

Greek symbols
δ fraction of bubbles in the bed, (−)
ΔP pressure drop, Pa
$\overline{\Delta P}Z$ average pressure drop during 60 s, Pa
ΔP_1 pressure drop in zone I, Pa
ΔP_2 pressure drop in zone II, Pa
ΔP_d total pressure drop across the distributor, Pa
ΔP_i pressure drop at time instant i, Pa
ε_1 voidage in zone I, (−)
ε_2 voidage ion zone II, (−)
$\varepsilon(t)$ bed voidage at any time t, (−)
ε_D dense phase voidage, (−)
ε_{mb} bed voidage at minimum bubbling velocity, (−)
ε_{mf} bed voidage at minimum fluidising velocity, (−)
ρ_b bulk density, kg/m^3
ρ_f gas density, kg/m^3
ρ_p particle density, kg/m^3
ρ_{tap} tapped density, kg/m^3
τ_{comp} compressibility time, s
τ_H bed height settling time, s
τ_P zero pressure drop time, s

References

[1] D. Geldart, A.L. Radtke, The effect of particle properties on the behaviour of equilibrium cracking catalyst in standpipe, Powder Technol. 47 (1986) 157–165.
[2] S. Bodin, C. Briens, M.A. Bergougnou, T. Patureaux, Standpipe flow modeling, experimental validation and design recommendations, Powder Technol. 124 (2002) 8–17.
[3] Y.M. Chen, Recent advances in FCC technology, Powder Technol. 163 (2006) 2–8.
[4] L.S. Leung, L.A. Wilson, Downflow of solids in standpipes, Powder Technol. 7 (1973) 343–349.
[5] E.T. Santos, R. Andreux, M. Hemati, G. Ferschneider, Influence of aeration taps spacing in standpipe flows, IFSA Industrial Fluidization South Africa Proceedings, 2008, pp. 282–298.
[6] E.T. Santos, Etude expérimentale et numérique du soutirage des particules d'un lit fluidisé. Application au cas industrial du FCC, PhD Thesis, Université de Toulouse, France, 2010.
[7] K. Rietema, Proc. Int. Symp. Fluidization, Eindhoven, 1967, 154.
[8] A.A.H. Drinkenburg, K. Rietema, Gas transfer from bubbles in a fluidized bed to the dense phase — II. Experiments, Chem. Eng. Sci. 28 (1973) 259–273.
[9] A.R. Abrahamsen, D. Geldart, Behaviour of gas-fluidized beds of fine powders Part II. Voidage of the dense phase in bubbling beds, Powder Technol. 26 (1980) 47–55.
[10] Y. Tung, M. Kwauk, China-Japan Symposium on Fluidization 49 (1982) 155.
[11] G.F. Barreto, J.G. Yates, P.N. Rowe, The measurement of emulsion phase voidage in gas fluidized beds of fine powders, Chem. Eng. Sci. 38 (1983) 345–350.
[12] G.F. Barreto, J.G. Yates, P.N. Rowe, The effect of pressure on the flow of gas in fluidized beds of fine particles, Chem. Eng. Sci. 38 (1983) 1935–1945.
[13] D. Geldart, C.Y. Wong, Fluidization of powders showing degrees of cohesiveness—II. Experiments on rates of de-aeration, Chem. Eng. Sci. 40 (1985) 653–661.
[14] G.F. Barreto, G.D. Mazza, J.G. Yates, The significance of bed collapse experiments in the characterization of fluidized beds of fine powders, Chem. Eng. Sci. 43 (1988) 3037–3047.
[15] J.J. Park, J.H. Park, I.S. Chang, S.D. Kim, C.S. Choi, A new bed-collapsing technique for measuring the dense phase properties of gas-fluidized beds, Powder Technol. 66 (1991) 249–257.
[16] P.G. Murfitt, P.L. Bransby, De-aeration of powders in hoppers, Powder Technol. 27 (1980) 149–162.
[17] P.N. Rowe, D.J. Chessmann, J. Yong, Y. Zhiquing, Proceedings of World Congress III Chemical Engineering (1986).
[18] D.S. Sharma, T. Pugsley, R. Delatour, Three-dimensional CFD model of the deareation rate of FCC particles, AIChE Journal 52 (2006) 2391–2400.
[19] P. Cherntongchai, S. Brandani, A model for the interpretation of the bed collapse experiment, Powder Technol. 151 (2005) 37–43.
[20] D. Geldart, Types of gas fluidisation, Powder Technol. 7 (1973) 285–292.
[21] J.F. Richardson, Fluidization, Academic Press, New York, 1971.
[22] S. Mori, C.Y. Wen, Flow estimation of bubble diameter in gaseous fluidised beds, AIChE Journal 21 (1975) 109–115.
[23] D. Geldart, C.Y. Wong, Fluidization of powders showing degrees of cohesiveness—I. Bed expansion, Chem. Eng. Sci. 39 (1984) 1481–1488.